CXCL4 signaling and gene induction in human monocytes involve a TLR4 response divergent from LPS

Chao Yang[1,*,#], Ruoxi Yuan[1], Bikash Mishra[1,3], Richard D. Bell[1], Yaxia Zhang[2,4], Yong Du[1], Marie Dominique Ah Kioon[1], Franck J. Barrat[1,3,5], Lionel B. Ivashkiv[1,3,6#]

[1]HSS Research Institute and David Z. Rosensweig Genomics Research Center and [2]Department of Pathology and Laboratory Medicine, Hospital for Special Surgery, New York, NY; [3]Immunology and Microbial Pathogenesis Program and [4]Department of Pathology and Laboratory Medicine and [5]Department of Microbiology and Immunology and [6]Department of Medicine, Weill Cornell Medicine, New York, NY.

[#] Correspondence: Chao Yang: ychmax@163.com; Lionel B. Ivashkiv: IvashkivL@hss.edu

[*]Current address: State Key Laboratory for Diagnosis and Treatment of Infectious Diseases, National Clinical Research Centre for Infectious Diseases, Collaborative Innovation Centre for Diagnosis and Treatment of Infectious Diseases, The First Affiliated Hospital, Zhejiang University School of Medicine, 79 Qingchun Rd., Hangzhou City, 310003, China.

Abstract

The chemokine CXCL4 activates myeloid cells and contributes to the pathogenesis of inflammatory and fibrotic diseases. One mechanism of CXCL4 action is binding of nucleic acids to promote their internalization and activation of endosomal TLRs. However, the signaling pathways and receptors that mediate myeloid cell responses to CXCL4 alone are not well characterized. Here, we report that in primary human monocytes, CXCL4 activated NF-κB and a TBK1-JNK signaling axis that drive the expression of inflammatory, fibrotic and neutrophil chemokine genes, and also RIPK3-dependent necroptosis. Surprisingly, six distinct lines of evidence targeting TLR4 expression and function suggested a role for TLR4 in CXCL4 responses. However, in contrast to the canonical TLR4 agonist LPS, CXCL4 did not effectively activate an autocrine IFN response or IL-12 family genes, even after IFN-γ priming of monocytes. In accord with its role in inducing chemokine and inflammatory gene expression, CXCL4 regulated neutrophil and macrophage infiltration into skin wounds, and promoted wound healing in a mouse model. Our findings suggest that CXCL4 modulates the profile of TLR4 responses to induce a macrophage phenotype divergent from LPS-activated cells, provide new insights into mechanisms by which CXCL4 activates human monocytes, and implicate CXCL4 in regulation of skin wound healing.

Main

Chemokine (C-X-C motif) ligand 4 (CXCL4), also known as platelet factor 4 (PF4), is a major product of platelets[1], and large amounts of CXCL4 are released at sites of tissue injury when platelets are activated and degranulate to initiate the coagulation process. CXCL4 is also expressed by immune cells at sites of inflammatory pathology, such as plasmacytoid dendritic cells (pDCs) in fibrotic skin lesions in systemic sclerosis (SSc)[2, 3] and macrophages in inflamed joint tissues in rheumatoid arthritis (RA)[4]. Accordingly, high levels of CXCL4 are found in skin wounds and are associated with multiple inflammatory conditions, including atherosclerosis, inflammatory bowel disease (IBD), SSc, and RA[2, 4, 5, 6]. CXCL4 can be present at concentrations as high as 10 μg/ml at sites of inflammation in IBD and 0.5 μg/ml in serum of SSc patients[2, 7, 8]. CXCL4 has been strongly implicated in inflammatory and related pro-fibrotic processes in SSc, primary myelofibrosis, and models thereof, where it can act on pDCs and endothelial, fibroblastic and myeloid cells[2, 3, 9, 10, 11].

CXCL4 has wide-ranging effects on myeloid cells including induction of reactive oxygen intermediates and inflammatory cytokines and chemokines[1, 12], macrophage differentiation[13] and polarization of conventional DCs into a pro-fibrotic phenotype that is hyper-responsive to stimulation with ligands of nucleic acid-sensing endosomal Toll-like receptors (TLR3 and TLR8) [3, 9, 14, 15]. The mechanism by which CXCL4 stimulates myeloid cells is not well understood; myeloid cells do not express CXCR3, the only known chemokine receptor for CXCL4, and myeloid cell activation by CXCL4 is independent of chemokine receptors and their associated G protein-mediated signaling pathways[1, 16]. One recently described mechanism by which CXCL4 activates cells independent of chemokine receptors is assembly of CXCL4 with “self” or microbial nucleic acids (NAs) into nanoparticles[1, 12, 17, 18], which facilitates internalization of

bound NAs to augment activation of endosomal NA-sensing Toll-like receptors (TLRs) such as TLR8/9 in pDCs and macrophages[7, 12, 18]. In human macrophages, formation of CXCL4-NA nanoparticles contributes to synergistic activation of inflammatory genes and of the NLRP3 inflammasome when cells are stimulated simultaneously with CXCL4 and a single stranded RNA TLR8 ligand[12].

Several groups including ours have reported activation of inflammatory signaling pathways and chromatin remodeling at inflammatory genes in myeloid cells after stimulation with CXCL4 alone, in the absence of exogenous nucleic acids[1, 10, 12, 14, 18]. This suggests that CXCL4 can also activate myeloid cells independently of its NA-chaperone properties. However, mechanistic understanding of myeloid cell activation by CXCL4 has been limited over several decades of investigation by the lack of a high affinity cognate receptor that mediates CXCL4 signaling events. Instead, CXCL4 binds to cells via low affinity charge-charge interactions with cell surface proteoglycans (PGs)[17]. In accord with a well-established model whereby PGs serve as co-receptors that facilitate interactions of various growth factors, chemokines, and cytokines with their receptors[19], PG-mediated presentation of CXCL4 to cell surface receptors such as LDLR and αMβ2 integrins has been proposed to mediate cell activation[20, 21]. Binding of CXCL4 to αMβ2 (also called Mac-1) changes cell morphology, shifts αMβ2 to an intracellular location co-localized with actin, and increases cell migration and phagocytosis[21]. However, the receptors and signaling pathways that mediate inflammatory activation of macrophages by CXCL4 are not well characterized.

Cell responses to bacterial lipopolysaccharide (LPS) are mediated by TLR4. TLR4 is expressed on the plasma membrane as part of a heterodimer with Myeloid Differentiation Protein-2 (MD-2), which is required for LPS sensing and cell activation. TLR4 forms only weak

and minimal contacts with LPS, and effective activation of TLR4 by LPS, which occurs at picomolar concentrations, requires MD-2 and additional LPS-binding proteins such as CD14 that act upstream of and sensitize responses to TLR4 (reviewed in [22]). CD14 binds and transfers LPS to MD-2, which results in TLR4 dimerization and activation of Myd88-mediated NF-κB and MAPK signaling. TLR4 subsequently traffics to endosomes, where its signaling is mediated by a distinct adaptor TRIF that, in addition to NF-κB and MAPKs, activates transcription factor IRF3 and downstream IFN responses. A role for TLR4 has also been proposed in the activation of macrophages by various endogenous proteins and proteoglycans that are released during cell death or degradation of extracellular matrix (termed DAMPs or alarmins) (reviewed in [23, 24]). Interactions between some DAMPs and TLR4 have been detected in the nanomolar range and by co-immunoprecipitation experiments, and one model proposes that these DAMPs work as ligands and direct agonists of TLR4. A different model proposes that these DAMPs may instead act by binding LPS and presenting it to TLR4/MD-2, thus sensitizing macrophages to respond to low LPS concentrations, similar to the function of CD14[23]. In this paradigm, LPS-binding DAMPs function as TLR4-sensitizing molecules, and this sensitization function can also occur in vivo, where DAMPs can bind LPS derived from the microbiome, or from bacteria present during bacteremia or at wound sites.

In our previous study of cooperation between CXCL4 and TLR8 in macrophage activation, we found that CXCL4 alone substantially activated NF-κB and MAPK signaling and weakly activated TANK-binding kinase 1 (TBK1), whereas TLR8 strongly activated interferon-regulated factors (IRFs) and synergized with CXCL4 to potently activate TBK1[12]. In the current study, we investigated mechanisms by which CXCL4 alone activates human monocytes, and the role of CXCL4 in regulating macrophage phenotype in a skin wound model. We found that NF-

□B and a TBK1-JNK signaling axis are important for induction of inflammatory and tissue repair/fibrotic genes by CXCL4, and CXCL4 also induced cell death in a RIPK3- and MLKL-dependent manner. Surprisingly, induction of inflammatory and fibrotic genes and related signaling pathways was strongly dependent on TLR4, but CXCL4 only minimally induced expression of interferon-stimulated genes (ISGs) and IL-12 family genes compared to the canonical TLR4 agonist LPS, which suggests that TLR4 becomes activated or signals in a noncanonical manner in the presence of CXCL4. In addition, deletion of CXCL4 altered infiltration of skin wounds by neutrophils and macrophage populations and delayed wound healing. These results identify mechanisms by which CXCL4 induces and regulates macrophage activation.

Results

CXCL4 activates inflammatory and tissue repair pathways in human monocytes

We used a transcriptomic approach to gain insight into how CXCL4 activates human monocytes. Our previous work[12] showed that CXCL4 rapidly but transiently induces expression of inflammatory genes such as *TNF* and *IL6*, with a return to near baseline 6 hours after CXCL4 stimulation. Here, we analyzed the transcriptomics of the CXCL4 response at 1 h and 3 h in human monocytes using RNA-seq (Extended Data Fig.1a). CXCL4 stimulation significantly (FDR < 0.05, fold change ≥ 2) upregulated expression of 1,771 genes and downregulated expression of 1,840 genes at 3 h (Fig. 1a). Various inflammatory and tissue repair/fibrotic genes were significantly upregulated, including *IL6*, *IL1B*, *TNF*, *CXCL1*, *PDGFA* and *PDGFB* (Fig. 1a). Significantly differentially expressed genes (DEGs) (4,004; FDR < 0.05, fold change ≥ 2) clustered into 4 groups based on pattern of expression (Fig. 1b). Genes in groups III and IV were early response-genes whose expression changed at 1 h after CXCL4 stimulation while changes in expression of genes in groups I and II were observed at 3 h (Fig. 1b). Gene-ontology (GO) and Ingenuity Pathway Analysis (IPA) analysis[25] of genes regulated by CXCL4 at 3 h showed most significant enrichment of cytokine-mediated signaling, immune response, apoptotic and wound healing/fibrosis pathways (Fig. 1c and 1d). Gene Set Enrichment Analysis (GSEA)[26, 27] further supported activation of wound healing and related TGF-β1 signaling and revealed enrichment of genes in myeloid cell differentiation and JNK signaling pathways (Fig. 1e and Extended Data Fig. 1c). CXCL4-mediated induction of representative inflammatory, fibrotic, and wound healing genes is shown in heatmaps (Fig. 1f and Extended Data Fig. 1d - f). Notably, CXCL4 induced expression of neutrophil chemokine genes CXCL1, CXCL2 and CXCL3 that are relevant for neutrophil infiltration into wound sites. CXCL4 still significantly induced *TNF* expression when

any endogenous extracellular DNA and RNA were depleted from cultures (Extended Data Fig. 2a), supporting that CXCL4 can activate cells independently of forming complexes with NAs. Overall, the data show that CXCL4 broadly activates inflammatory and profibrotic gene expression, and induces neutrophil chemokine genes, in human monocytes.

NF-κB and a TBK1-JNK axis drive inflammatory, fibrotic and neutrophil chemokine gene expression

CXCL4 alone substantially activates NF-κB and MAPKs p38 and ERK, and also activates TBK1[12]. We next investigated the role of these signaling molecules in induction of representative inflammatory and fibrotic genes, and the neutrophil chemokines CXCL1 and CXCL2. Activation of NF-κB was dependent on IKKα/β and TAK1 (Extended Data Fig. 3a), and as expected, inhibition of IKKα/β suppressed CXCL4-induced expression of canonical inflammatory NF-κB target genes *IL6*, *TNF*, *IL1B* and *IRF1* (Extended Data Fig. 3b). Strikingly, induction of representative wound healing/fibrotic genes *PDGFA* and *PDGFB* was essentially completely blocked by NF-κB inhibition, while induction of *CXCL1* and *CXCL2* was relatively resistant (Extended Data Fig. 3c). These results implicate NF-κB in the regulation of fibrotic in addition to inflammatory genes in CXCL4-stimulated monocytes.

We next confirmed activation of TBK1 by CXCL4 alone in an additional 3 donors (Fig. 2a). In human monocytes activation of TBK1 is coupled with induction of inflammatory NF-κB target genes[12, 28]. Accordingly, three different TBK1 inhibitors suppressed CXCL4-mediated induction of inflammatory genes *TNF* and *IL1B* (Fig. 2b). Induction of fibrotic genes *PDGFA*, *PDGFB* and *CXCL1* was suppressed, while *IL6* and *IRF1* were not affected (Fig. 2b and

Extended Data Fig. 4a). As inhibition of TBK1 does not diminish NF-κB activation[12], we tested whether TBK1 regulates MAPK signaling. In addition to activating ERK and p38[12], CXCL4 activated MAPK JNK p46 and p54 isoforms, and this activation was suppressed when TBK1 was inhibited (Fig. 2c). CXCL4 also activated the upstream MAPK kinases MKK4/7 that phosphorylate and activate JNK in canonical MAPK signaling pathways[29]. However, CXCL4-induced MKK4/7 phosphorylation was not sensitive to TBK1 inhibitors (Extended Data Fig. 4b), suggesting TBK1 can activate JNK by a noncanonical pathway. In accord with this notion, JNK co-immunoprecipitated with TBK1 in unstimulated human monocytes, which suggests that TBK1 interacts with JNK even in the steady state; CXCL4 stimulation did not consistently increase the interaction of JNK with TBK1 (Fig. 2d and Extended Data Fig. 4c).

Next, we evaluated the contribution of JNK to CXCL4-induced gene expression. Inhibition of JNK significantly suppressed CXCL4-mediated induction of *TNF*, *IL1B, PDGFB* and *CXCL1* (Fig. 2e and Extended Data Fig. 4d). A role for JNKs in CXCL4-induced gene expression was corroborated using siRNA-mediated knockdown of both JNK1 and JNK2 (Fig. 2f, g and Extended Data Fig. 4e). The effects of inhibiting ERKs and p38 were more limited than inhibition of JNKs (Extended Data Fig. 5). Collectively, these data highlight the importance of a CXCL4-activated TBK1-JNK axis in induction of key inflammatory, fibrotic and neutrophil chemokine genes.

CXCL4 activates STAT3 via IL-10 autocrine signaling

CXCL4 could activate STAT3, as assessed by phosphorylation at tyrosine 705 (Extended Data Fig. 6a). Inflammatory factors typically activate Jak-STAT signaling indirectly via induction of

cytokines that function in an autocrine manner. In accord with this model, inhibition of cytokine secretion using Brefeldin A (BFA) abolished CXCL4-inducedSTAT3 activation. The STAT3-activating cytokine IL-10 was induced by CXCL4 (Extended Data Fig. 6b, c) and blockade of IL-10 function using IL-10Rα neutralizing antibody completely abolished CXCL4-induced STAT3 phosphorylation (Extended Data Fig. 6d). Although autocrine IL-10 downregulates inflammatory gene [30, 31], knockdown of STAT3 using siRNA (Extended Data Fig. 6e) had minimal effect on CXCL4-induced *IL6*, *TNF*, *IL1B*, and *IRF1* expression (Extended Data Fig. 6g), possibly because of low amounts of endogenous IL-10 or incomplete STAT3 knockdown. However, STAT3 knockdown significantly decreased induction of the known STAT target gene *PIM1* and of *PDGFA* (Extended Data Fig. 6f); in contrast, induction of *CXCL1* and *CXCL2* were increased. These results implicate STAT3 in CXCL4-mediated gene regulation and suggest that STAT3 can play a positive role in induction of fibrotic genes in addition to its established role in monocytes of suppressing inflammatory responses.

CXCL4 regulates neutrophil and macrophage infiltration and promotes healing of skin wounds

We hypothesized that CXCL4 plays a role in the early phase of wound healing, after platelet degranulation, and during the inflammatory phase days 1-3 post wounding when neutrophils and macrophages infiltrate the wound site. We used flow cytometry to track neutrophils, macrophages and fibroblasts in a full thickness dorsal excisional skin wound model[32]; the gating strategy is shown in Extended Data Figure 7a. 2 days after wounding, the proportion of neutrophils in *Cxcl4*$^{-/-}$ mice was significantly reduced compared to WT mice (Fig. 3a and Extended Data Fig. 7b), which is in accord with a role for CXCL4 in inducing neutrophil

chemokine expression. In line with a previous study[33], macrophages could be separated into Ly6C^{hi}F4/80^{dim} and Ly6C^{dim}F4/80^{hi} subpopulations (Fig. 3b, left panel). Deletion of *Cxcl4* significantly increased the proportion of Ly6C^{hi}F4/80^{dim} relative to Ly6C^{dim}F4/80^{hi} macrophages (Fig. 3b and Extended Data Fig. 7c). This data suggests that CXCL4 contributes to macrophage activation and differentiation in vivo[13, 34]. In accord with a previous study[33], Ly6C^{dim}F4/80^{hi} macrophages showed much greater CD64 and CD206 cell-surface expression compared to Ly6C^{hi}F4/80^{dim} macrophages (Fig. 3c and Extended Data Fig. 8a), which is consistent with a more differentiated macrophage phenotype. Additionally, Ly6C^{dim}F4/80^{hi} macrophages showed higher intracellular staining for phosphorylated TBK1 and JNK than did Ly6C^{hi}F4/80^{dim} macrophages (Fig. 3d and Extended Data Fig. 8a). CXCL4 also resulted in a trend towards decreased fibroblasts in wounds without affecting fibroblast proliferation (Fig. 3e, f).

To gain additional insight into the functional phenotype of these macrophage populations we performed RNAseq using purified flow-sorted Ly6C^{hi}F4/80^{dim} and Ly6C^{dim}F4/80^{hi} macrophages from skin wounds (Extended Data Fig. 9a, b). Notably, *Cxcl4* was more highly expressed in Ly6C^{dim}F4/80^{hi} compared to Ly6C^{hi}F4/80^{dim} macrophages (Extended Data Fig. 9a) Pathway analysis showed that Ly6C^{hi}F4/80^{dim} macrophages express an inflammatory phenotype, whereas Ly6C^{dim}F4/80^{hi} macrophages showed highest enrichment of genes involved in metabolic pathways, PPAR signaling and cell replication (Extended Data Fig. 9c, d), which is consistent with an alternatively activated phenotype that promotes wound closure. Differential expression of representative inflammatory and wound healing genes in these two macrophage populations is depicted in Extended Data Fig. 9e. These data suggest a proinflammatory role for Ly6C^{hi}F4/80^{dim} whereas Ly6C^{dim}F4/80^{hi} macrophages may be alternative activated macrophages, which play important roles in remodeling and regulating fibroblasts to close the wound[35, 36, 37, 38].

To assess the functional consequences of *Cxcl4* deletion on wound healing, we tracked the rate of wound healing over 7 days through daily time-lapse planimetric measurements. Wounds from *Cxcl4*$^{-/-}$ mice closed at a significantly delayed pace in first 4 days and were eventually comparable to WT or heterozygous *Cxcl4*$^{+/-}$ controls in the late stage (Fig. 3g and Extended Data Fig. 8c). Collectively, the data show that on day 2 after wounding, CXCL4 promotes neutrophil infiltration while altering the ratios of inflammatory and homeostatic macrophages, and these changes are temporally associated with improved wound healing.

CXCL4 activates a TRIF-utilizing receptor to induce RIPK3-dependent necroptosis

Only a relatively small subset of inflammatory factor receptors can activate RIPK3 and downstream necroptotic cell death - TNF receptor family members that contain a death domain and activate RIPK3 via RIPK1, and receptors that utilize the TRIF signaling adaptor (namely, TLR3 and TLR4) and can activate RIPK3 directly. To try to narrow down the receptor(s) that CXCL4 engages to induce inflammatory responses, we tested whether CXCL4 induces RIPK3-mediated necroptosis, which is mediated by downstream effector MLKL and requires inhibition of Caspase-8 to prevent inactivating cleavage of RIPK3[39]. Stimulation of monocytes with CXCL4 in the presence of the Caspase inhibitor Z-VAD-FMK (zVAD) resulted in a significant induction of cell death (Fig. 4a). CXCL4-induced cell death was significantly blocked by inhibition of MLKL using necrosulfonamide (NSA) (Fig. 4a) and by siRNA-mediated knockdown of RIPK3 or MLKL (Fig. 4b and Extended Data Fig. 10a). In contrast, knockdown of RIPK1 using siRNA did not reduce cell death (Fig. 4c and Extended Data Fig. 10b); the dispensability of RIPK1 makes upstream involvement of TNF family receptors less likely. Furthermore, neutralizing TNF antibodies and TNFR1 blocking antibodies did not reduce

CXCL4-induced cell death (Fig. 4d), arguing against a role for autocrine TNF. Additionally, degradation of extracellular nucleic acids in culture supernatants did not affect CXCL4-induced cell death (Fig. 4e), suggesting that CXCL4 did not induce cell death by promoting NA internalization. Finally, we tested the role of the signaling adaptor TRIF, which activates RIPK3 and contributes to TLR3/4-mediated necroptosis[40, 41, 42]. siRNA-mediated knock down of TRIF almost completely abolished CXCL4-induced necroptosis (Fig. 4f). These data suggest that CXCL4 activates a TRIF-utilizing receptor.

CXCL4 minimally activates IFN responses and IL-12 genes and is resistant to IFN priming in a gene-specific manner

To our knowledge, the only receptors that utilize TRIF for signaling are TLR3 and TLR4[22], and TRIF links these receptors to strong IFN responses mediated by induction of autocrine IFN-β that binds to its receptor IFNAR to activate Jak-STAT signaling and expression of interferon-stimulated genes (ISGs). We thus tested whether CXCL4 similarly induces an IFN response and as a comparator used the canonical TLR4 agonist LPS, which activates a robust IFN autocrine loop via TRIF-mediated signaling. CXCL4 induced expression of inflammatory genes *TNF* and *IL1B* comparably to LPS (5 ng/ml) (Fig. 5a). In striking contrast, CXCL4 minimally induced expression of ISGs *CXCL10* and *IFIT1* (Fig. 5a); the amounts of CXCL10 and IFIT1 mRNA induced by CXCL4 were at least two orders of magnitude lower than those induced by LPS. Induction of *IFNB* mRNA by CXCL4 was also lower than induction by LPS (Fig. 5a and 6b). Induction of ISGs by CXCL4 was mediated by autocrine IFNs as ISG induction was abolished by blocking antibodies to IFNAR2 (Fig. 5b), but induction of ISGs by CXCL4 was massively lower than induction of ISGs by exogenous IFN-α (Fig. 5b). Collectively these results indicate

that although CXCL4 activates inflammatory gene expression comparably to LPS, CXCL4 only minimally induces an IFN response.

Another distinction between CXCL4 and TLR4 responses was weak induction of *IL6* and *IL12B* and *IL12A* (Fig. 5c). A core feature of the LPS response in human monocytes is that induction of NF-κB target genes like *IL6* and *IL12B* is increased by pretreatment of cells with IFN-γ (termed priming)[43]. As expected, IFN-γ priming strongly increased the amounts of *TNF*, *IL6*, *IL1B*, *IFNB*, *IL12B* and *IL12A* mRNA induced by LPS (Fig. 5d and e). IFN-γ priming also increased the amounts of *TNF* mRNA induced by CXCL4 (Fig. 5d). In striking contrast, the amounts of *IL6*, *IL1B* and *IFNB* mRNA induced by CXCL4 were minimally increased by IFN-γ priming, and induction of *IL12B* and *IL12A* genes remained refractory to CXCL4 stimulation even in IFN-γ-primed macrophages (Fig. 5e). Thus, the difference between CXCL4 and LPS in responsiveness to IFN-γ priming was gene-specific, and the divergence of CXCL4 and LPS responses was supported by a preliminary transcriptomic analysis. Collectively, these results underscore the differences between CXCL4 and LPS in gene induction and responsiveness to IFN-γ priming.

CXCL4 signaling and gene activation involve TLR4

Since CXCL4 activates a TRIF-dependent necroptosis pathway, we considered known receptors that use TRIF as an adaptor, TLR3 and TLR4, as candidates for mediating the effects of CXCL4. TLR3 is minimally expressed in human macrophages[44] and stimulation of human macrophages with the TLR3 ligand poly (I:C) does not induce gene expression[12]. Thus, despite the differences between CXCL4 and LPS responses described above, we tested whether TLR4 is involved in

CXCL4 responses in human macrophages. The small molecule inhibitor of TLR4 signaling CLI-095 that binds to the TLR4 intracellular domain abolished both CXCL4- and LPS-induced expression of *TNF*, *IL1β* and *IL6* (Extended Data Fig. 11a). As a specificity control, CLI-095 did not affect gene induction by TLR2 ligand Pam3CSK4 (Extended Data Fig. 11b). In our recent study, we showed that the very low amount of LPS present in recombinant CXCL4 (1-2 pg/ml final concentration in experiments) does not have the ability to activate expression of inflammatory genes in human macrophages[12], and we found similarly low concentrations of LPS in additional lots of CXCL4 (Extended Data Fig. 12). Furthermore, CXCL4 completely lost its activity upon heat denaturation of proteins (Fig. 6a and Extended Data Fig. 11c), further supporting that the low concentrations of LPS contaminating CXCL4 preparations are insufficient to activate TLR4 on their own.

To further investigate whether TLR4 plays a role in CXCL4 responses, we blocked TLR4 using a specific neutralizing antibody and found that TLR4 blockade nearly completely abolished induction of inflammatory, fibrotic and neutrophil chemokine genes by both CXCL4 and LPS (Fig. 6b and Extended Data Fig. 11d). Although induction of *IFNB* by CXCL4 was lower than induction by LPS, the effects of both stimuli were strongly suppressed by TLR4 blockade (Fig. 6b). Further, genetic knockdown of TLR4 using its specific siRNA corroborated the role of TLR4 in CXCL4-induced gene expression in human macrophages (Fig. 6c and Extended Data Fig. 11e). Finally, we stimulated *Tlr4*$^{-/-}$ bone marrow-derived mouse macrophages (BMDMs) with human CXCL4 (hCXCL4) and found that deletion of *Tlr4* abolished CXCL4-induced gene expression (Fig. 6d). In accord with decreased gene induction, blockade of TLR4 using neutralizing antibodies or knockdown of TLR4 using siRNA suppressed CXCL4-induced TBK1 and NF-κB activation (Fig. 6e-h), and also abolished CXCL4-induced necroptosis (Fig.

6i and j). These studies provide four independent lines of evidence implicating TLR4 in mediating macrophage responses to CXCL4.

CXCL4 colocalizes with TLR4 and MD-2

Next, we investigated whether CXCL4 colocalized with TLR4. To do so, we treated human primary macrophages with CXCL4 for 30 min and the cells were fixed and stained with anti-CXCL4 and anti-TLR4 antibodies for immunofluorescence analysis. Addition of CXCL4 altered TLR4 staining to a more discrete pattern that colocalized with CXCL4, likely in intracellular compartments (Fig. 7a and Extended Data Fig. 13a). Myeloid Differentiation factor 2 (MD-2) associates with TLR4 and is requisite for LPS signaling via TLR4[45, 46]. MD-2 also colocalized with CXCL4 in human macrophages after 30 min stimulation with CXCL4 (Fig. 7b and Extended Data Fig. 13b). Inhibition of MD-2 using MD2-IN-1[47] abolished both CXCL4 and LPS-induced gene expression (Fig. 7c). These data suggest that CXCL4 and the TLR4/MD-2 complex traffic to similar intracellular compartments after CXCL4 stimulation of human macrophages, where TLR4-TRIF signaling can be activated, and provide an additional two lines of evidence supporting a role for TLR4 in CXCL4 responses.

Discussion

The importance of CXCL4 in inflammatory disease pathogenesis is well established, especially for inflammation-associated fibrosis in SSc[48, 49]{van Bon, 2014 #117}{Ah Kioon, 2018 #351}{Lande, 2019 #311}{Affandi, 2022 #524}, but the mechanisms by which CXCL4 activates cells are not well defined. Our understanding of how this chemokine activates inflammatory instead of chemotactic responses has been hampered by lack of knowledge of which receptor(s) mediate CXCL4-induced inflammatory responses, and limited characterization of CXCL4-activated signaling pathways. This study advances the field in three ways. First, we have identified that CXCL4 induces a TBK1-JNK signaling axis that complements NF-κB in activating inflammatory, fibrotic and neutrophil chemokine genes; hence, this work highlights a role for TBK1 distinct from its established function in activating IFN responses. CXCL4 also activates STAT3 and RIPK3 that are important in regulating inflammatory responses and cell death. Second, in accord with a role in chemokine gene induction, we have identified an in vivo function of CXCL4 in promoting neutrophil infiltration, regulating macrophage populations, and promoting skin wound healing. Finally, we found that CXCL4 responses were dependent on TLR4, but that CXCL4 induces a gene expression profile distinct from that induced by LPS, suggesting that CXCL4 modulates TLR4 responses. These findings provide new insights into the functions and mechanisms of action of CXCL4, and suggest a new paradigm by which a chemokine can activate macrophages.

Although a role for TLR4 in monocyte responses to CXCL4 is unexpected, we have provided 6 distinct lines of evidence supporting this notion: 1. Sensitivity of CXCL4 responses to a small molecule TLR4 inhibitor. 2. Inhibition of CXCL4 responses by a TLR4 blocking antibody. 3. Attenuation of CXCL4 responses by siRNA-mediated knockdown of TLR4. 4. Loss

of CXCL4-induced gene expression by genetic deletion of *Tlr4*. 5. Attenuation of CXCL4 responses by an MD-2 inhibitor. 6. Colocalization of CXCL4 with TLR4 and MD-2. Collectively, these results make it unlikely that the role of TLR4 is related to off-target or nonspecific effects of the inhibitors or genetic approaches that were used. It is possible that binding of CXCL4 at the plasma membrane by PGs[12], which increases local CXCL4 concentrations, promotes low affinity interactions with TLR4 and/or MD-2, similar to CXCL4 interactions with the LDLR and CD11b/CD18 previously described[20, 21]. As CXCL4 belongs to the subgroup of chemokines that can self-aggregate[50], CXCL4 aggregates could crosslink TLR4 and initiate signaling and internalization. In this model, CXCL4 would act as a TLR4 'agonist', as has been proposed for a various endogenous proteins that are DAMPs or alarmins, such as biglycan, hyaluronin, versican, tenascin-C, fibrinogen, heat shock proteins, HMGB1, β-defensins and LDLs[23, 24]. The possibility that CXCL4 is a direct TLR4 agonist would require extensive validation in future work using biochemical and structural biology approaches with purified proteins.

Another non-mutually exclusive and equally interesting possibility about how TLR4 is activated in our system is based on observations that many of the endogenous proteins suggested to activate TLR4, including heat shock proteins, surfactant protein A, β-defensins, fibrinogen, biglycan and LDLs can bind and/or enhance the sensitivity of cells to LPS in a manner analogous to CD14[23]. In this model, these alarmins serve as enhancers of LPS sensing, rather than direct agonists of TLR4. In our system, addition of CXCL4 to cell cultures resulted in only extremely low LPS concentrations (1-2 pg/ml), which is not sufficient to activate monocytes when LPS alone added to such cultures[12]. Although LPS-binding by proteins can suppress the readout of the LAL assay, the complete loss of bioactivity after heating CXCL4 solutions at 100 ^{o}C for 10 minutes to denature CXCL4 supports the importance of CXCL4 itself in eliciting the monocyte

response. The heat denaturation step did not inactivate LPS, as this requires dry heat ('burning') at >250 ^{o}C for > 30 min. A function for CXCL4 as a sensitizer of monocyte responses to LPS would be particularly relevant in scenarios such as very early wounds where CXCL4 is provided by platelet degranulation and low numbers of bacteria are present. Such a role would expand the conceptualization of CXCL4 as a sensitizer of TLRs7/8/9 in several cell types via NA binding to a broader role in the sensitization of additional TLR responses in myeloid cells. Notably, the CXCL4-induced signaling and gene induction events observed herein in monocytes were not observed in pDCs or B cells (Ref[18] and unpublished data), which express minimal TLR4 levels and are much less sensitive to TLR4 ligands.

Regardless of exactly how TLR4 is engaged by CXCL4, the transcriptional output after CXCL4 stimulation differed from the transcriptional output of TLR4 activation by LPS, most notably a negligible IFN response and lack of activation of IL-12 family genes by CXCL4. A difference in macrophage signaling and transcriptional responses to an endogenous putative TLR4 agonist and LPS has been previously described for tenascin-C[51]. Similar to CXCL4, tenascin-C was not able to activate IL-12 family genes; IFN responses were not analyzed in this previous study. As TLR responses and the balance between inflammatory and IFN responses are affected by intracellular trafficking through endolysosomal compartments[22, 52], it is possible that altered trafficking of TLR4 after CXCL4 stimulation, as suggested by Figure 7, affected the IFN response by modulating the intensity or duration of IRF activation and 'repurposing' TBK1 for inflammatory gene induction. Alternatively, signaling crosstalk with the additional receptors engaged by CXCL4, such as CD11b/CD18, LDLRs and cell surface PGs[12, 17, 20, 21], could affect TLR4-mediated transcriptional output. CD11b/CD18 is well established to modulate TLR4 signaling in a complex manner[53]{Wang, 2010 #642}. Overall, these findings suggest an

important function for CXCL4 in the modulation of TLR responses that is important for calibrating immune and inflammatory responses.

CXCL4, TLR8 and TLR4 have been shown to play important roles in tissue fibrosis in diseases such as SSc[3, 54, 55]{Gleissner, 2010 #404}{Affandi, 2022 #524}{van Bon, 2014 #117} and can affect the activation and function of various pathogenic cell types. One pathogenic function of CXCL4 in SSc is to promote NA-mediated activation of TLR8 and TLR9 in plasmacytoid DCs[3, 18]{Gleissner, 2010 #404}. A key role for TLR4 in SSc pathogenesis has been established by the efficacy of TLR4 inhibitors or genetic deletion of *Tlr4* in ameliorating disease in preclinical models[54, 55]. In contrast to NA-mediated activation of TLR8, in SSc TLR4 is activated by endogenous protein 'agonists' including tenacin-C, fibronectin-EDA, HMGB1 and S100 proteins. Our findings suggest that the high concentrations of CXCL4 present in SSc may also contribute to pathogenesis by activation, either directly or indirectly, of TLR4.

In summary, CXCL4 activation of human monocytes involves TLR4 and NF-κB and TBK1-JNK signaling pathways that drive inflammatory and tissue repair/fibrotic gene expression distinct from TLR4 activation by LPS. CXCL4 also activates expression of neutrophil chemokine genes and regulates neutrophil and macrophage recruitment and healing of skin wounds. These findings provide insights about how CXCL4 can contribute to inflammatory and fibrotic disease pathogenesis, and suggest strategies for targeting CXCL4-activated pathways to suppress pathology.

Methods

Human cells

Deidentified human buffy coats were purchased from the New York Blood Center following a protocol approved by the Hospital for Special Surgery Institutional Review Board. Peripheral blood mononuclear cells (PBMCs) were isolated using density gradient centrifugation with Lymphoprep (Accurate Chemical, Carle Place, NY, USA) and monocytes were purified with anti-CD14 magnetic beads from PBMCs immediately after isolation as recommended by the manufacturer (Miltenyi Biotec)[56]. Monocytes were cultured overnight at 37°C, 5% CO_2 in RPMI-1640 medium (Invitrogen) supplemented with 10% heat-inactivated defined FBS (HyClone Fisher), penicillin-streptomycin (Invitrogen), L-glutamine (Invitrogen) and 20 ng/ml human M-CSF. Then, the cells were treated as described in the figure legends.

Mice

Animal experiments were approved by the Weill Cornell Medicine IACUC Committee. C57BL/6J mice (Strain #:000664) and *Tlr4*$^{-/-}$ mice (Strain #:029015) at 6 to 8 weeks old were purchased from the Jackson Laboratories. *Cxcl4*$^{-/-}$ mice at 6 weeks old were obtained from Dr. M. Anna Kowalska at the Children's Hospital of Philadelphia. C57BL/6J mice were crossed with *Cxcl4*$^{-/-}$ mice to generate *Cxcl4*$^{+/-}$ mice. *Cxcl4*$^{+/-}$ male mice were crossed with female *Cxcl4*$^{+/-}$ mice and/or female *Cxcl4*$^{-/-}$ mice to generate either WT, *Cxcl4*$^{+/-}$ or *Cxcl4*$^{-/-}$ mice as littermate controls. Littermate controls were used except as noted in figure legends. All the mice were housed under specific pathogen-free conditions.

Skin wound healing

Full-thickness wounds were created by excision of 4-mm punches on either side of midline[32]. Four wounds were generated in the upper back of mice for flow cytometry analysis of cellular proportions; 2 wounds were generated in the upper and lower back of mice for cell sorting and wound closure experiments. Prior to the surgery, age- and sex-matched, randomly assigned mice were anesthetized with isoflurane and subcutaneous injections of buprenorphine (0.5 mg/kg) were given as analgesics. Wound areas were measured by tracing onto a glass slide at the indicated time points. Slides were scanned and area calculated with ImageJ. At the indicated time points, mice were euthanized, and wound tissues were collected with 8-mm biopsy punches.

Mouse bone marrow-derived macrophage (BMDM) culture.

Bone marrow cells from male C57BL/6J mice and male *Tlr4*$^{-/-}$ mice were harvested after euthanasia by CO2 asphyxiation, and cultured in RPMI-1640 medium (Invitrogen) supplemented with 10% heat-inactivated defined FBS (HyClone Fisher), penicillin-streptomycin (Invitrogen), L-glutamine (Invitrogen) and 20 ng/ml mouse M-CSF 6 days. Then, the cells were treated as described in the figure legends.

RNA sequencing

Libraries for sequencing were prepared using extracted RNA and the NEBNext Ultra II RNA Library Prep Kit for Illumina following the manufacturer's instructions (New England Biolabs). Quality of all RNA and library preparations were evaluated with BioAnalyzer 2100 (Agilent). Human RNA libraries were sequenced by the Genomics Resources Core Facility at Weill Cornell using a HiSeq4000, 50-bp single-end reads at a depth of –at least 20 million uniquely mapped reads per sample. Mouse RNA libraries were sequenced using NovaSeq 6000, 50-bp paired-end reads at a depth of at least 20 million uniquely mapped reads per sample. Read

quality was assessed and adapters trimmed using Fastp. Reads were then mapped to the human genome (hg38) and mouse genome (mm10) and reads in exons were counted against Gencode M25 with STAR Aligner. Differential gene expression analysis was performed in R using edgeR. Genes with low expression levels (< 3 counts per million in at least one group) were filtered from all downstream analyses. Benjamini-Hochberg false discovery rate (FDR) procedure was used to correct for multiple testing.

Analysis of mRNA amounts

Total RNA was extracted with a RNeasy Mini Kit (QIAGEN) and was reverse-transcribed with a RevertAid RT Reverse Transcription Kit (Thermo Fisher Scientific, Catalog number: K1691). Real-time PCR was performed with Fast SYBR Green Master Mix and a 7500 Fast Real-time PCR system (Applied Biosystems). The primer sequences for the qPCR reactions are listed in Extended Data Table 1. CT values of target genes were normalized to *GAPDH* expression and are shown as percentage of GAPDH ($100/2^{\Delta Ct}$).

Western Blotting

Cells were lysed in 50 µl of cold buffer containing 50 mM Tris-HCl pH 7.4, 150 mM NaCl, 1 mM EDTA, 1% (vol/vol) Triton X-100, 2 mM Na3VO4, 1x phosSTOP EASYPACK, 1 mM Pefabloc, and 1× EDTA-free complete protease inhibitor cocktail (Roche, Basel, Switzerland), and incubated for 10 min on ice. Then, cell debris was pelleted at 13,000 rpm at 4°C for 10 min. The soluble protein fraction was mixed with 4× Laemmli Sample buffer (BIO-RAD, Cat. #1610747) and 2-mercroptoehanol (BME) (Sigma-Aldrich). Samples for Western blotting were subjected to electrophoresis on 4–12% Bis-Tris gels (Invitrogen). Proteins were transferred to polyvinylidene difluoride membrane was as previously reported[57]. Membranes were blocked in 5%

(w/v) Bovine Serum Albumin in TBS (20 mm Tris, 50 mm NaCl, pH 8.0) with 0.1% (v/v) Tween 20 (TBST) at room temperature for at least 1 h with shaking at 60 rpm. Membranes were then incubated with primary antibodies at 4 °C overnight with shaking at 60 rpm. Membranes were washed 3 times in TBST, then probed with anti-mouse or anti-rabbit IgG secondary antibodies conjugated to horseradish peroxidase (GE Healthcare, cat: NA9310V and NA9340V) diluted in TBST at room temperature for one hour with shaking at 60 rpm. Next, membranes were washed 3 times in TBST at room temperature for with shaking at 60 rpm. Antibody binding was detected using enhanced chemiluminescent substrates for horseradish peroxidase (HRP) (ECL Western blotting reagents (PerkinElmer, cat: NEL105001EA) or SuperSignal West Femto Maximum Sensitivity Substrate (Thermo Fisher Scientific, cat: 34095), according to the manufacturer's instructions, and visualized using premium autoradiography film (Thomas Scientific, cat: E3018). To detect multiple proteins on the same experimental filter, membranes were cut horizontally based on the molecular size of the target proteins. For membranes that required probing twice or more using different primary antibodies, RestoreTM PLUS Western blotting stripping buffer (Thermo Fisher Scientific) was applied on the blots with shaking at 60 rpm for 15 min following previous development. Antibodies used are identified in Extended Data Table 2.

Immunoprecipitation

Human monocytes (20 x 10^6) were lysed in 650 µl of IP Lysis/Wash buffer (Pierce Direct IP Kit, Thermo Fisher Scientific, Cat. #26148) and the supernatants of cell lysates after centrifugation were transferred to columns containing the TBK1 antibody linked to AminoLink Plus Coupling Resin to pull down the proteins interacting with TBK1 using the Pierce Direct IP Kit according to the manufacturer’s instructions. The immunoprecipitated proteins were denatured with 4×

Laemmli Sample buffer and BME and boiled for 5 min, resolved by SDS-PAGE and immunoblotted with indicated antibodies.

Cytokine detection by ELISA

Levels of IL-6, TNF and IL-1β were determined in supernatants of cells using enzyme-linked immunosorbent assay (ELISA) kits (R&D biosystems) according to the manufacturer's instructions.

RNA interference

For RNA interference (RNAi) experiments, primary human monocytes (6 x 10^6 cells) were transfected with 0.1 nmol of siRNA oligonucleotides (listed in Extended Data Table 3) using a Human Monocyte Nucleofactor Kit (Lonza, VVPA-1007) and the AMAXA Nucleofector System (Lonza) program Y001 for human monocyte transfection according to the manufacturer's instructions.

Flow cytometric (FACS) analysis

Wounded skin samples were minced and digested with DNase I (80µg/ml) and collagenase IV (370U/ml) in RPMI-1640 medium supplemented with 10% BSA at 37 shaking at 200 rpm for 45 min in a shaker. Cells were centrifuged to remove digestion buffer and red blood cells were lysed with ACK lysing buffer (Lonza, cat# 10-548E) for 5 min. After washing with FACS buffer (PBS containing 2% calf serum and 1 mM EDTA), cells were then filtered with 70 µm cell strainer and stained with LIVE/DEAD Fixable Blue Dead Cell Stain Kit (Thermo Fisher Scientific, cat# L23105) and Fc blocking antibody (BD Pharmingen, cat# 553141) in PBS. After washing with PBS, cells in each sample were then equally divided into two parts for either immune cell staining or stromal cell staining. The antibodies used for immune cell staining

include F4/80, Ly6C, CD64, Ly6G, CCR2, CD206, phospho-JNK, phosphor-TBK1, CD11b and CD45; the antibodies used for stromal cell staining include ki67, α-SMA, Ter119, PDGFRα/CD140α CD31 and CD45. Antibodies used in this study are listed in Extended Data Table 2. After washing, the cells were analyzed using BD FACSymphony A3 Cell Analyzer and Flowjo software.

Endotoxin detection

The concentration of endotoxin in CXCL4 stock solutions was measured by Chromogenic LAL Endotoxin Assay Kit (GenScript, cat. No: L00350C) according to the manufacturer's instructions.

Skin macrophage sorting

Wounded skin cells were prepared following the method described in the Flow cytometric (FACS) analysis section. The cells from 2 – 3 mice were pooled together and stained with antibodies including F4/80, Ly6C, Ly6G, CD11b and CD45. Before sorting DAPI was added to the cells to label the dead cells. Cells were sorted using Becton-Dickinson Aria II. After sorting, the cells were quickly lysed with buffer RLT (QIAGEN, cat# 79216).

Confocal microscopy

The protocol was as described in our previous publication[58]. Briefly, human monocytes were cultured in 20 ng/ml M-CSF for 3 to 6 days and incubated with 10 μg/ml human CXCL4 for 30 min, fixed in PBS buffer containing 4% paraformaldehyde at room temperature (RT) for 15 min, and permeabilized for 10 min with 0.1 % Triton-X 100 in PBS. Samples were then blocked by 3% BSA in PBS for 30 min at RT, and labeled with anti-CXCL4-PE (1:50) (R&D system, IC7952P) and anti-TLR4 (10 μg/ml) (R&D system, AF1478), or anti-MD-2 (2 μg/ml) (Thermo Fisher Scientific, PA5-20058) for 3 h at RT. Secondary antibodies (1:1000) anti-goat-AF647 (1:1000)

(Thermo Fisher Scientific, A-21446) or anti-rabbit CF647 (1:1000) (Sigma, SAB4600175) are used when needed. Images were acquired using a ZEISS LSM880 confocal microscope and a 63×/1.4 N.A. objective.

Statistical Analysis

Graphpad Prism for Windows was used for all statistical analysis. Information about the specific tests used, and number of independent experiments is provided in the figure legends. Two-way ANOVA with Sidak correction for multiple comparisons was used for grouped data; when the data did not pass normality distribution by the Shapiro-Wilk test, the Friedman test with Dunn's correction was used. Otherwise, one-way ANOVA with the Geisser-Greenhouse correction and Tukey's post hoc test for multiple comparisons was performed. For paired data, when the data did not pass the normal distribution by F test the Wilcoxon signed-rank test was performed, otherwise, paired t test was used.

Data availability

The RNAseq data sets that support the findings of this study and were generated by the authors as part of this study have been deposited in the Gene Expression Omnibus database with the accession code: GSE210105. Otherwise, the data is either contained within the manuscript or available from the authors on request.

Acknowledgments

We thank the Weill Cornell Medicine Genomics Core Facility for next generation sequencing, the Weill Cornell Medicine – HSS Flow Cytometry Core Facility for flow cytometry support, and David Oliver (HSS Genomics Center) for advice and discussions. This work was supported by NIH grants R01 AI044938, R01 AR46713 and R01 AR050401 (L.B.I.). F.J.B. is supported by grants from the NIH 1R01AI132447, from the Scleroderma Research Foundation and from the

Scleroderma Foundation. The David Z. Rosensweig Genomics Center at HSS is supported by The Tow Foundation. All NIH-supported work was performed at HSS.

Author contributions

C.Y. conceptualized, designed, and performed most of the experiments, performed bioinformatic analysis, prepared figures and wrote the manuscript. R.Y., B. M., R. B., Y. Z., Y. D., M.D.A.K., contributed experiments or experimental expertise; F.J.B. contributed expertise and intellectual input and edited the manuscript. L.B.I. conceptualized and oversaw the study and edited the manuscript. All authors reviewed and provided input on the manuscript.

Competing interests

F.J.B. is a founder of IpiNovyx, a startup biotechnology company.

References:

1. Kasper, B. & Petersen, F. Molecular pathways of platelet factor 4/CXCL4 signaling. *European Journal of Cell Biology* **90**, 521-526 (2011).

2. van Bon, L. *et al.* Proteome-wide analysis and CXCL4 as a biomarker in systemic sclerosis. *N Engl J Med* **370**, 433-443 (2014).

3. Ah Kioon, M.D. *et al.* Plasmacytoid dendritic cells promote systemic sclerosis with a key role for TLR8. *Sci Transl Med* **10** (2018).

4. Yeo, L. *et al.* Expression of chemokines CXCL4 and CXCL7 by synovial macrophages defines an early stage of rheumatoid arthritis. *Ann Rheum Dis* **75**, 763-771 (2016).

5. Meuwis, M.-A. *et al.* Biomarker discovery for inflammatory bowel disease, using proteomic serum profiling. *Biochemical pharmacology* **73**, 1422-1433 (2007).

6. Ridiandries, A., Tan, J.T.M. & Bursill, C.A. The Role of Chemokines in Wound Healing. *Int J Mol Sci* **19** (2018).

7. Lande, R. *et al.* CXCL4 assembles DNA into liquid crystalline complexes to amplify TLR9-mediated interferon-alpha production in systemic sclerosis. *Nat Commun* **10**, 1731 (2019).

8. Meuwis, M.A. *et al.* Biomarker discovery for inflammatory bowel disease, using proteomic serum profiling. *Biochemical pharmacology* **73**, 1422-1433 (2007).

9. Silva-Cardoso, S.C. *et al.* CXCL4 Exposure Potentiates TLR-Driven Polarization of Human Monocyte-Derived Dendritic Cells and Increases Stimulation of T Cells. *J Immunol* **199**, 253-262 (2017).

10. Gleitz, H.F.E. *et al.* Increased CXCL4 expression in hematopoietic cells links inflammation and progression of bone marrow fibrosis in MPN. *Blood* **136**, 2051-2064 (2020).

11. Affandi, A.J. *et al.* CXCL4 drives fibrosis by promoting several key cellular and molecular processes. *Cell Reports* **38**, 110189 (2022).

12. Yang, C. *et al.* CXCL4 synergizes with TLR8 for TBK1-IRF5 activation, epigenomic remodeling and inflammatory response in human monocytes. *Nature Communications* **13**, 3426 (2022).

636 13. Domschke, G. & Gleissner, C.A. CXCL4-induced macrophages in human atherosclerosis. *Cytokine*
637 (2017).

638
639 14. Silva-Cardoso, S.C. *et al.* CXCL4 Links Inflammation and Fibrosis by Reprogramming Monocyte-
640 Derived Dendritic Cells in vitro. *Front Immunol* **11**, 2149 (2020).

641
642 15. Silva-Cardoso, S.C. *et al.* CXCL4 suppresses tolerogenic immune signature of monocyte-derived
643 dendritic cells. *Eur J Immunol* **50**, 1598-1601 (2020).

644
645 16. Gleissner, C.A. Macrophage Phenotype Modulation by CXCL4 in Atherosclerosis. *Front Physiol* **3**,
646 1 (2012).

647
648 17. Rauova, L. *et al.* Monocyte-bound PF4 in the pathogenesis of heparin-induced
649 thrombocytopenia. *Blood* **116**, 5021-5031 (2010).

650
651 18. Du, Y. *et al.* Chemokines form nanoparticles with DNA and can superinduce TLR-driven immune
652 inflammation. *Journal of Experimental Medicine* **219** (2022).

653
654 19. Frey, H., Schroeder, N., Manon-Jensen, T., Iozzo, R.V. & Schaefer, L. Biological interplay between
655 proteoglycans and their innate immune receptors in inflammation. *Febs j* **280**, 2165-2179 (2013).

656
657 20. Sachais, B.S. *et al.* Platelet factor 4 binds to low-density lipoprotein receptors and disrupts the
658 endocytic itinerary, resulting in retention of low-density lipoprotein on the cell surface. *Blood* **99**,
659 3613-3622 (2002).

660
661 21. Lishko, V.K., Yakubenko, V.P., Ugarova, T.P. & Podolnikova, N.P. Leukocyte integrin Mac-1
662 (CD11b/CD18, αMβ2, CR3) acts as a functional receptor for platelet factor 4. *Journal of*
663 *Biological Chemistry* **293**, 6869-6882 (2018).

664
665 22. Fitzgerald, K.A. & Kagan, J.C. Toll-like Receptors and the Control of Immunity. *Cell* **180**, 1044-
666 1066 (2020).

667
668 23. Erridge, C. Endogenous ligands of TLR2 and TLR4: agonists or assistants? *Journal of Leukocyte*
669 *Biology* **87**, 989-999 (2010).

670
671 24. Frey, H., Schroeder, N., Manon-Jensen, T., Iozzo, R.V. & Schaefer, L. Biological interplay between
672 proteoglycans and their innate immune receptors in inflammation. *The FEBS Journal* **280**, 2165-
673 2179 (2013).

674
675 25. Breuer, K. *et al.* InnateDB: systems biology of innate immunity and beyond--recent updates and
676 continuing curation. *Nucleic Acids Res* **41**, D1228-1233 (2013).

677
678 26. Subramanian, A. *et al.* Gene set enrichment analysis: A knowledge-based approach for
679 interpreting genome-wide expression profiles. *Proceedings of the National Academy of Sciences*
680 **102**, 15545-15550 (2005).

681
682 27. Mootha, V.K. *et al.* PGC-1α-responsive genes involved in oxidative phosphorylation are
683 coordinately downregulated in human diabetes. *Nature Genetics* **34**, 267-273 (2003).

684
685 28. Heinz, L.X. *et al.* TASL is the SLC15A4-associated adaptor for IRF5 activation by TLR7-9. *Nature*
686 **581**, 316-322 (2020).

687
688 29. Haeusgen, W., Herdegen, T. & Waetzig, V. The bottleneck of JNK signaling: molecular and
689 functional characteristics of MKK4 and MKK7. *Eur J Cell Biol* **90**, 536-544 (2011).

690
691 30. Ip, W.K.E., Hoshi, N., Shouval, D.S., Snapper, S. & Medzhitov, R. Anti-inflammatory effect of IL-10
692 mediated by metabolic reprogramming of macrophages. *Science* **356**, 513-519 (2017).

693
694 31. Murray, P.J. The primary mechanism of the IL-10-regulated antiinflammatory response is to
695 selectively inhibit transcription. *Proceedings of the National Academy of Sciences* **102**, 8686-
696 8691 (2005).

697
698 32. Kusnadi, A. *et al.* The Cytokine TNF Promotes Transcription Factor SREBP Activity and Binding to
699 Inflammatory Genes to Activate Macrophages and Limit Tissue Repair. *Immunity* **51**, 241-257
700 e249 (2019).

701
702 33. Crane, M.J. *et al.* The monocyte to macrophage transition in the murine sterile wound. *PLoS One*
703 **9**, e86660 (2014).

704
705 34. van der Kroef, M. *et al.* CXCL4 triggers monocytes and macrophages to produce PDGF-BB,
706 culminating in fibroblast activation: Implications for systemic sclerosis. *J Autoimmun* **111**,
707 102444 (2020).

708
709 35. Boniakowski, A.E. *et al.* Murine macrophage chemokine receptor CCR2 plays a crucial role in
710 macrophage recruitment and regulated inflammation in wound healing. *Eur J Immunol* **48**, 1445-
711 1455 (2018).

712
713 36. Gonzalez, A.C., Costa, T.F., Andrade, Z.A. & Medrado, A.R. Wound healing - A literature review.
714 *An Bras Dermatol* **91**, 614-620 (2016).

715

716 37. Krzyszczyk, P., Schloss, R., Palmer, A. & Berthiaume, F. The Role of Macrophages in Acute and
717 Chronic Wound Healing and Interventions to Promote Pro-wound Healing Phenotypes. *Front*
718 *Physiol* **9**, 419 (2018).

719
720 38. Vannella, K.M. & Wynn, T.A. Mechanisms of Organ Injury and Repair by Macrophages. *Annu Rev*
721 *Physiol* **79**, 593-617 (2017).

722
723 39. He, S. & Wang, X. RIP kinases as modulators of inflammation and immunity. *Nature Immunology*
724 **19**, 912-922 (2018).

725
726 40. Najjar, M. *et al.* RIPK1 and RIPK3 Kinases Promote Cell-Death-Independent Inflammation by Toll-
727 like Receptor 4. *Immunity* (2016).

728
729 41. He, S., Liang, Y., Shao, F. & Wang, X. Toll-like receptors activate programmed necrosis in
730 macrophages through a receptor-interacting kinase-3–mediated pathway. *Proceedings*
731 *of the National Academy of Sciences* **108**, 20054-20059 (2011).

732
733 42. Kaiser, W.J. *et al.* Toll-like receptor 3-mediated necrosis via TRIF, RIP3, and MLKL. *The Journal of*
734 *biological chemistry* **288**, 31268-31279 (2013).

735
736 43. Qiao, Y. *et al.* Synergistic activation of inflammatory cytokine genes by interferon-gamma-
737 induced chromatin remodeling and toll-like receptor signaling. *Immunity* **39**, 454-469 (2013).

738
739 44. Heinz, S. *et al.* Species-specific regulation of Toll-like receptor 3 genes in men and mice. *J Biol*
740 *Chem* **278**, 21502-21509 (2003).

741
742 45. Shimazu, R. *et al.* MD-2, a molecule that confers lipopolysaccharide responsiveness on Toll-like
743 receptor 4. *The Journal of experimental medicine* **189**, 1777-1782 (1999).

744
745 46. Hamann, L. *et al.* A coding mutation within the first exon of the human MD-2 gene results in
746 decreased lipopolysaccharide-induced signaling. *Genes Immun* **5**, 283-288 (2004).

747
748 47. Zhu, S. *et al.* Anti-inflammatory effects of α7-nicotinic ACh receptors are exerted through
749 interactions with adenylyl cyclase-6. *Br J Pharmacol* **178**, 2324-2338 (2021).

750
751 48. Kania, G., Rudnik, M. & Distler, O. Involvement of the myeloid cell compartment in fibrogenesis
752 and systemic sclerosis. *Nature Reviews Rheumatology* **15**, 288-302 (2019).

753
754 49. Volkmann, E.R. & Varga, J. Emerging targets of disease-modifying therapy for systemic sclerosis.
755 *Nature Reviews Rheumatology* **15**, 208-224 (2019).

50. Hughes, C.E. & Nibbs, R.J.B. A guide to chemokines and their receptors. *Febs j* **285**, 2944-2971 (2018).

51. Piccinini, A.M., Zuliani-Alvarez, L., Lim, J.M. & Midwood, K.S. Distinct microenvironmental cues stimulate divergent TLR4-mediated signaling pathways in macrophages. *Sci Signal* **9**, ra86 (2016).

52. Blasius, A.L. & Beutler, B. Intracellular Toll-like Receptors. *Immunity* **32**, 305-315 (2010).

53. Ling, G.S. *et al.* Integrin CD11b positively regulates TLR4-induced signalling pathways in dendritic cells but not in macrophages. *Nat Commun* **5**, 3039 (2014).

54. Bhattacharyya, S. *et al.* TLR4-dependent fibroblast activation drives persistent organ fibrosis in skin and lung. *JCI Insight* **3** (2018).

55. Brown, M. & O'Reilly, S. Innate immunity and Toll-like receptor signaling in the pathogenesis of scleroderma: advances and opportunities for therapy. *Curr Opin Rheumatol* **30**, 600-605 (2018).

56. Huynh, L. *et al.* Opposing regulation of the late phase TNF response by mTORC1-IL-10 signaling and hypoxia in human macrophages. *Scientific Reports* **6**, 31959 (2016).

57. Yang, C. *et al.* IFNgamma receptor down-regulation facilitates Legionella survival in alveolar macrophages. *J Leukoc Biol* **107**, 273-284 (2020).

58. Guiducci , C. *et al.* Properties regulating the nature of the plasmacytoid dendritic cell response to Toll-like receptor 9 activation. *Journal of Experimental Medicine* **203**, 1999-2008 (2006).

Figure Legends:

Figure 1. (a) Volcano plot of DEGs regulated by CXCL4 (10 µg/ml) after 3 h treatment of human primary macrophages. (b) k-means clustering of the DEGs regulated in human primary macrophages by CXCL4 after 1 h and 3 h treatments (n = 3 independent donors). (c) Gene Ontology analysis using program InnateDB of DEGs regulated in human primary macrophages by CXCL4 after 3 h treatment. (d) IPA analysis of DEGs regulated in human primary macrophages by CXCL4 after 1 h and 3 h treatments. (e) GSEA analysis of DEGs after CXCL4 3 h treatment. (f) Heatmap of inflammatory genes regulated by CXCL4.

Figure 2. (a) Immunoblot of phospho-TBK1 and TBK1 with whole cell lysates of cells stimulated with CXCL4 for 1 h (n = 3 independent donors). (b) mRNA of *TNF*, *IL1β*, *PDGFA*, *PDGFB* and *CXCL1* measured by qPCR and normalized relative to *GAPDH* mRNA in cells pre-treated with TBK1/IKKε inhibitors MRT67307 HCl (10 µM), TBK1/IKKε-IN-2 (1 µM) or GSK8612 (50 µM) for 30 min and then stimulated with CXCL4 for 3 h (n = 5 independent donors). (c) Immunoblot of phospho-JNK (p54 and p46) and total JNK with whole cell lysates of cells pre-treated with TBK1/IKKε inhibitors MRT67307 HCl (10 µM), TBK1/IKKε-IN-2 (1 µM) or GSK8612 (50 µM) for 30 min and then stimulated with CXCL4 for 1 h (representative of 4 independent donors). (d) Immunoblot of TBK1 and JNK from whole cell lysates immunoprecipitated with TBK1 antibodies (representative of 5 independent donors). (e) mRNA of indicated genes measured by qPCR and normalized relative to *GAPDH* mRNA in cells pre-treated with JNK inhibitor SP600125 (10 µM) for 30 min and then stimulated with CXCL4 for 3 h (n = 5 independent donors). (f) Immunoblot of phospho-JNK and JNK using whole cell lysates 3 days after nucleofection of monocytes with control or JNK-specific siRNAs (representative of 3 independent donors). (g) mRNA of indicated genes was measured by qPCR and normalized

relative to *GAPDH* mRNA after knockdown of JNK by siRNA for 3 days (n = 6 independent donors). Data are depicted as mean ± SEM (b, e, g). **p ≤ 0.01; *p ≤ 0.05 by One-way ANOVA (b, e) or Two-way ANOVA (g). Source data are provided as a Source Data file.

Figure 3. (a, b,) FACS to analyze neutrophils (a) and macrophage subgroups (b) in the wounds of WT and *Cxcl4*$^{-/-}$ mice on day 2 after wounding. Left panels, representative FACS plots; right panels, cumulative data from two independent experiments performed in early 2022 (n = 8 for WT mice, 8 for *Cxcl4*$^{-/-}$ mice). (c, d) MFI from FACS experiments of CD64 and CD206 (c, data collected from 7 mice), phospho-TBK1 and phospho-JNK (d, data collected from 6 mice for P-TBK1 and from 7 mice for P-JNK) in indicated cell types. (e) FACS to analyze fibroblasts in the wounds of WT mice and *Cxcl4*$^{-/-}$ mice day 2 after wounding. Left panel, representative FACS plot; right panel, cumulative data (n = 7 for WT mice, 6 for *Cxcl4*$^{-/-}$ mice). (f) MFI of Ki67 staining in fibroblasts from c. (g) Wound closure in *Cxcl4*$^{-/-}$ and *Cxcl4*$^{+/-}$ mice over 7 dpi (n = 16 wounds of 4 mice for *Cxcl4*$^{+/-}$, 15 wounds of 4 mice for *Cxcl4*$^{-/-}$; littermate controls were used). Data are depicted as mean ± SEM. **p ≤ 0.01; *p ≤ 0.05 by unpaired t test, two-tailed (a, e), One-way ANOVA (c, d) or Two-way ANOVA (b, g). Source data are provided as a Source Data file.

Figure 4. (a) Cell death assay of human macrophages stimulated with CXCL4 in the presence/absence of Caspase-8 inhibitor zVAD (50 μM) and necrosulfonamide (NSA, 0.5 μM) for 6 h (n = 4 independent donors). (b) Cell death assay performed 3 days after nucleofection of monocytes with control (Ctrl) siRNA, RIPK3 or MLKL specific siRNAs, and then stimulated with CXCL4 in the presence/absence of Caspase-8 inhibitor zVAD for 6 h (n = 4 independent donors). (c, f) Cell death assay performed 3 days after nucleofection of monocytes with control (Ctrl) siRNA, RIPK1 (c) or TRIF (f) specific siRNAs, and then stimulated with CXCL4 in the presence/absence of Caspase-8 inhibitor zVAD for 6 h (n = 3 (c) or 4 (f) independent donors). (d,

e) Cell death assay in cells pretreated with TNF (n = 4 independent donors) or TNFR1 (n = 2 independent donors) neutralizing antibodies (d), or with DNase I (1000 U) + RNase A (50 ug/ml) (n = 3 independent donors) (e) for 1 h and then stimulated with CXCL4 in the presence of zVAD for 6 h. Data are depicted as mean ± SEM. ***p ≤ 0.001; **p ≤ 0.01; *p ≤ 0.05 by One-way ANOVA (a) or Two-way ANOVA (b, e, f). Source data are provided as a Source Data file.

Figure 5. (a, c) mRNA of indicated genes measured by qPCR and normalized relative to *GAPDH* mRNA in cells stimulated with LPS (5 ng/ml) or CXCL4 for 3 h (n = 4 independent donors).(b) mRNA of *CXCL10* and *ISG15* measured by qPCR and normalized relative to *GAPDH* mRNA in cells pre-treated with IFNAR2 neutralizing antibody (10 µg/ml) for 1 h and then stimulated with CXCL4 for 3 h (n = 3 independent donors). (d, e) mRNA of indicated genes measured by qPCR and normalized relative to *GAPDH* mRNA in cells pretreated with IFNγ (100 U/ml) for 24 h and then stimulated with LPS (5 ng/ml) or CXCL4 for 3 h (n = 4 independent donors). The data in a, c, d, and e are derived from the same donors and the resting, LPS and CXCL4 conditions in a, c, d and e represent the same samples; data are depicted separately to enhance visualization of the comparison of samples performed in the absence of IFN-γ in a and c. Data are depicted as mean ± SEM. ***p ≤ 0.001; **p ≤ 0.01; *p ≤ 0.05 by Two-way ANOVA. Source data are provided as a Source Data file.

Figure 6. (a) mRNA of *TNF* and *IL1B* measured by qPCR and normalized relative to *GAPDH* mRNA in cells treated with CXCL4 or heat denatured CXCL4 for 3 h (n = 4 independent donors). (b) mRNA of *TNF* and *IFNB* measured by qPCR and normalized relative to *GAPDH* mRNA in cells pre-treated with TLR4 neutralizing antibody (5 µg/ml) for 1 h and then stimulated with CXCL4 or LPS (5 ng/ml) for 3 h (n = 6 independent donors). (c) mRNA of indicated genes was measured by qPCR and normalized relative to *GAPDH* mRNA in cells after

knockdown of TLR4 by specific siRNA for 3 days and then stimulation with CXCL4 for 3 h (n = 4 independent donors). (d) mRNA of indicated genes was measured by qPCR and normalized relative to *GAPDH* mRNA in WT and *Tlr4*$^{-/-}$ BMDMs stimulated with CXCL4 for 3 h (n = 4 independent experiments). (e, f) Immunoblot of phospho-TBK1 and TBK1 with whole cell lysates of cells pre-treated with TLR4 neutralizing antibody (e) for 1 h or after knockdown of TLR4 by specific siRNA (f) for 3 days and then stimulated with CXCL4 for 3 h (representative of 4 independent donors for both e and f). (g, h) Immunoblot of phospho-p65 and p65 with whole cell lysates of cells pre-treated with TLR4 neutralizing antibody (g) for 1 h or after knockdown of TLR4 by specific siRNA (h) for 3 days and then stimulated with CXCL4 for 3 h (representative of 4 independent donors for both g and h). (i, j) Cell viability in cells pre-treated with TLR4 neutralizing antibody (i) for 1 h or after knockdown of TLR4 by specific siRNA (j) for 3 days and then stimulation with CXCL4 in the presence/absence of zVAD for 3 h (n = 3 independent donors for both i and j). Data are depicted as mean ± SEM (a - d, i and j). ****$p \leq 0.0001$; ***$p \leq 0.001$; **$p \leq 0.01$; *$p \leq 0.05$ by One-way ANOVA (a) or Two-way ANOVA (b - d, i and j). Source data are provided as a Source Data file.

Figure 7. (a, b) Confocal microscopy images of CXCL4 colocalization with TLR4 (a) and MD-2 (b) in human macrophages 30 min after treatment (representative images from 3 independent experiments with different donors for each TLR4 and MD-2). (c) mRNA of *IL6* and *TNF* measured by qPCR and normalized relative to *GAPDH* mRNA in cells pre-treated with MD-2 inhibitor MD2-IN-1 (10 μM) for 30 min and then stimulated with CXCL4 or LPS (5 ng/ml) for 3 h (n = 3 independent donors). Data are depicted as mean ± SEM (c). Source data are provided as a Source Data file.

Yang et al., Fig. 1

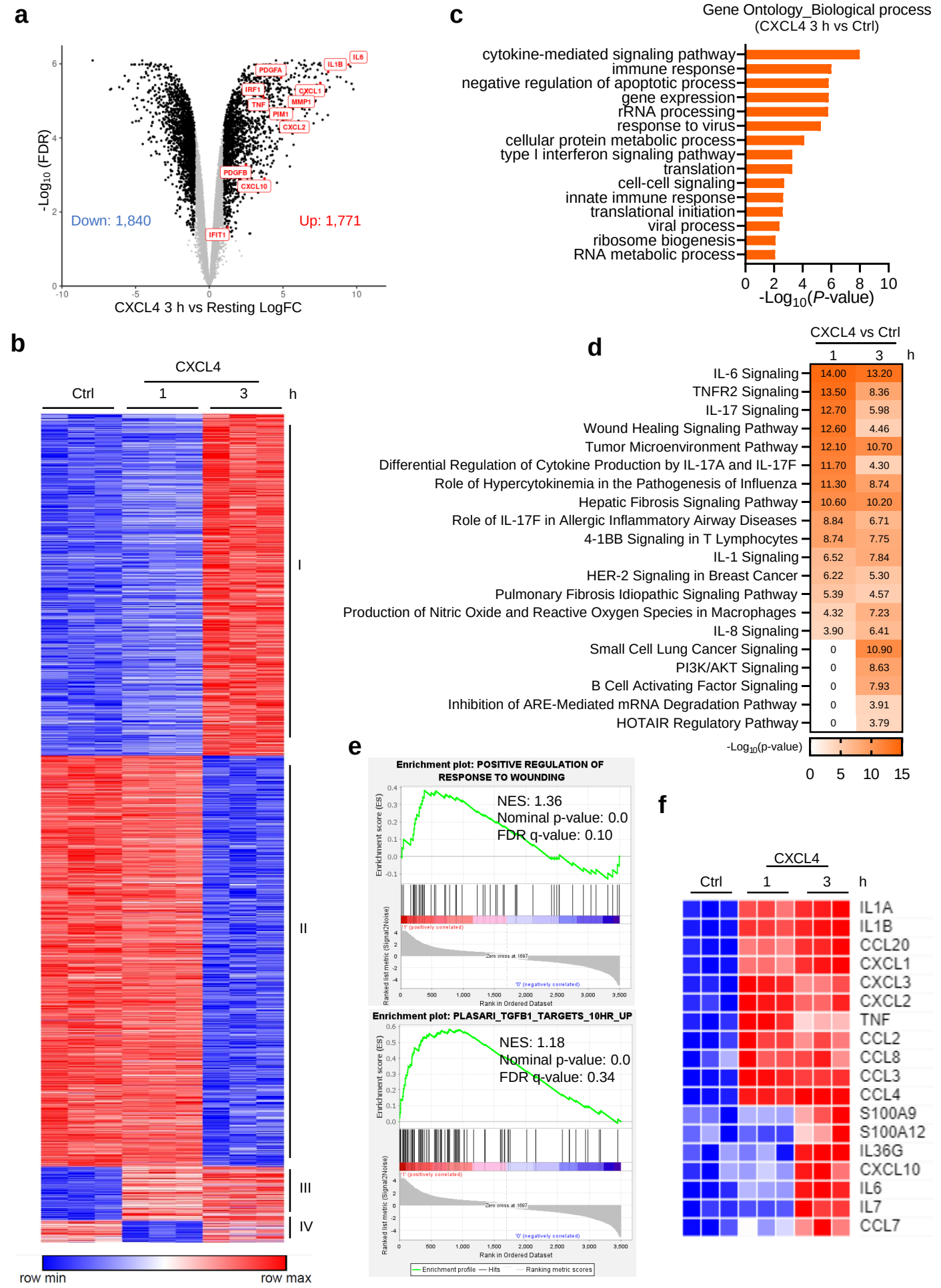

Yang et al., Fig. 2

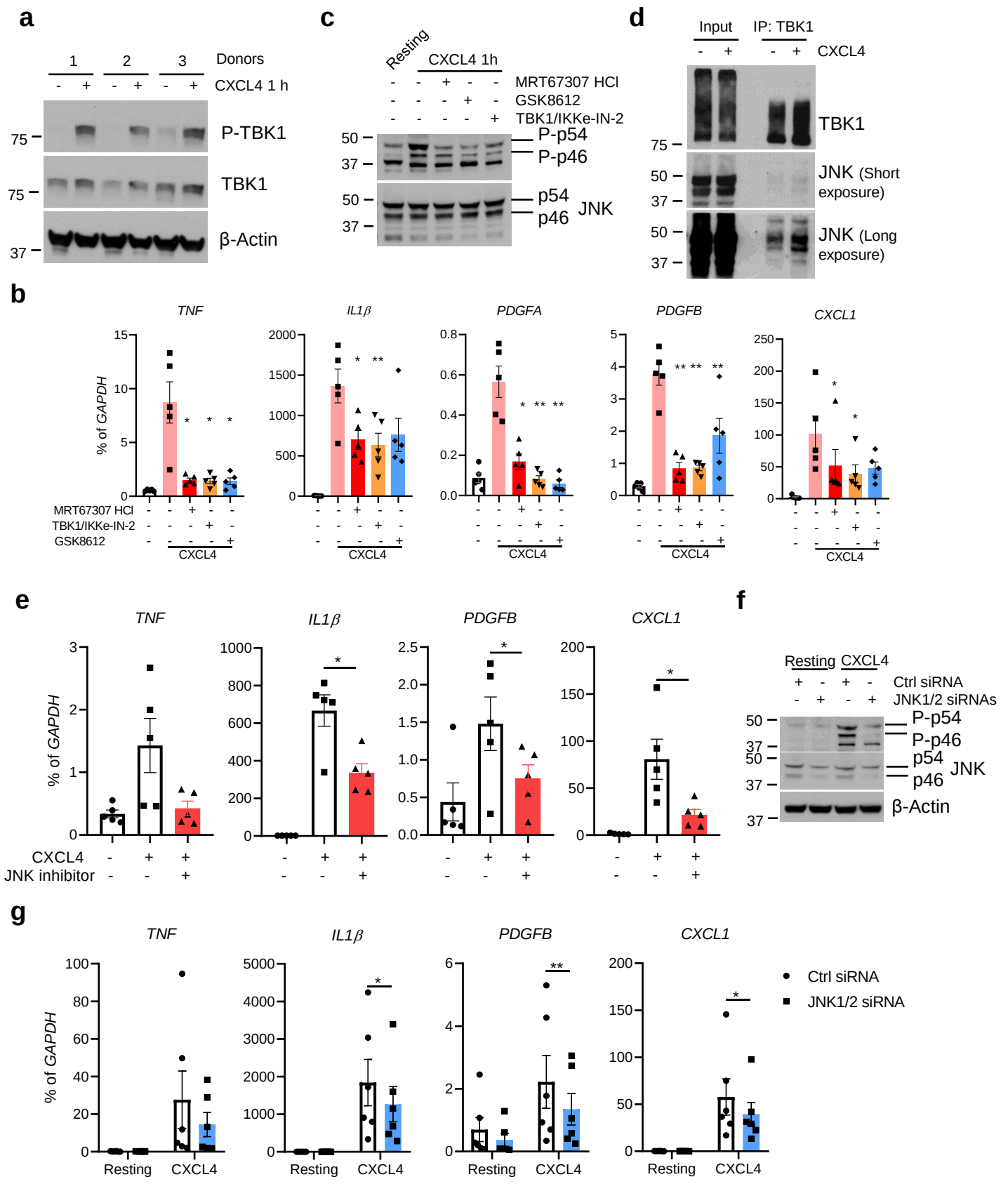

Yang et al., Fig. 3

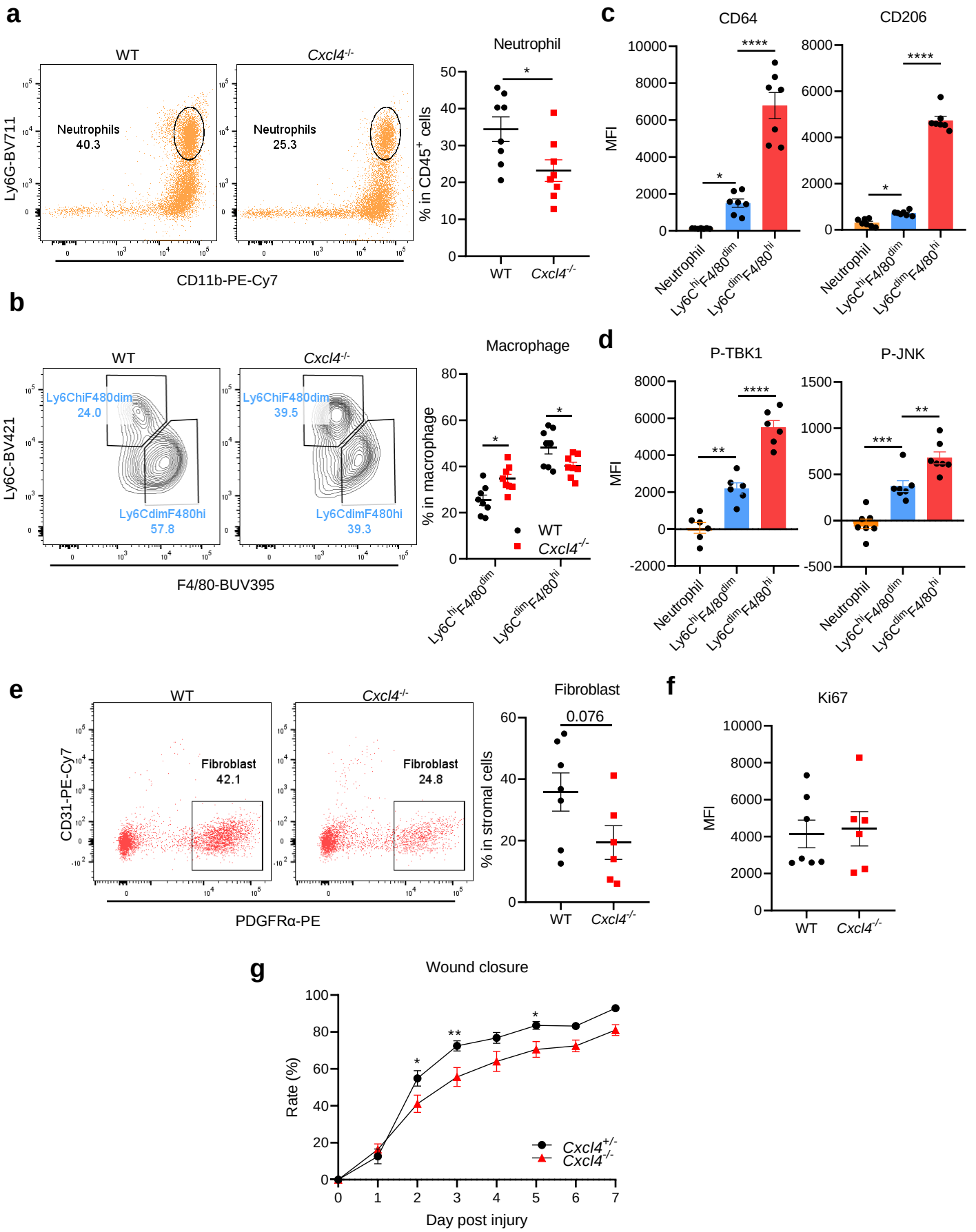

Yang et al., Fig. 4

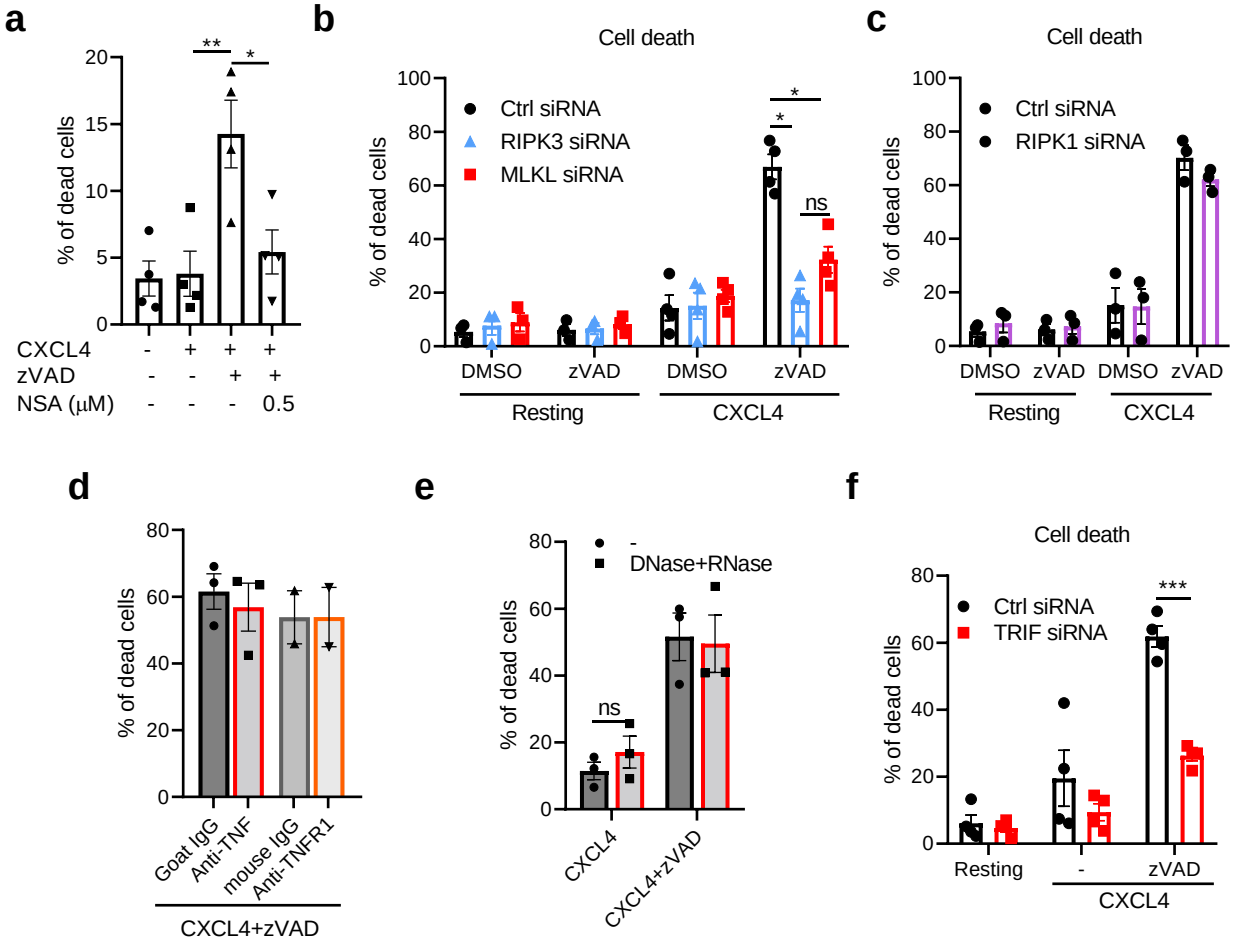

Yang et al., Fig. 5

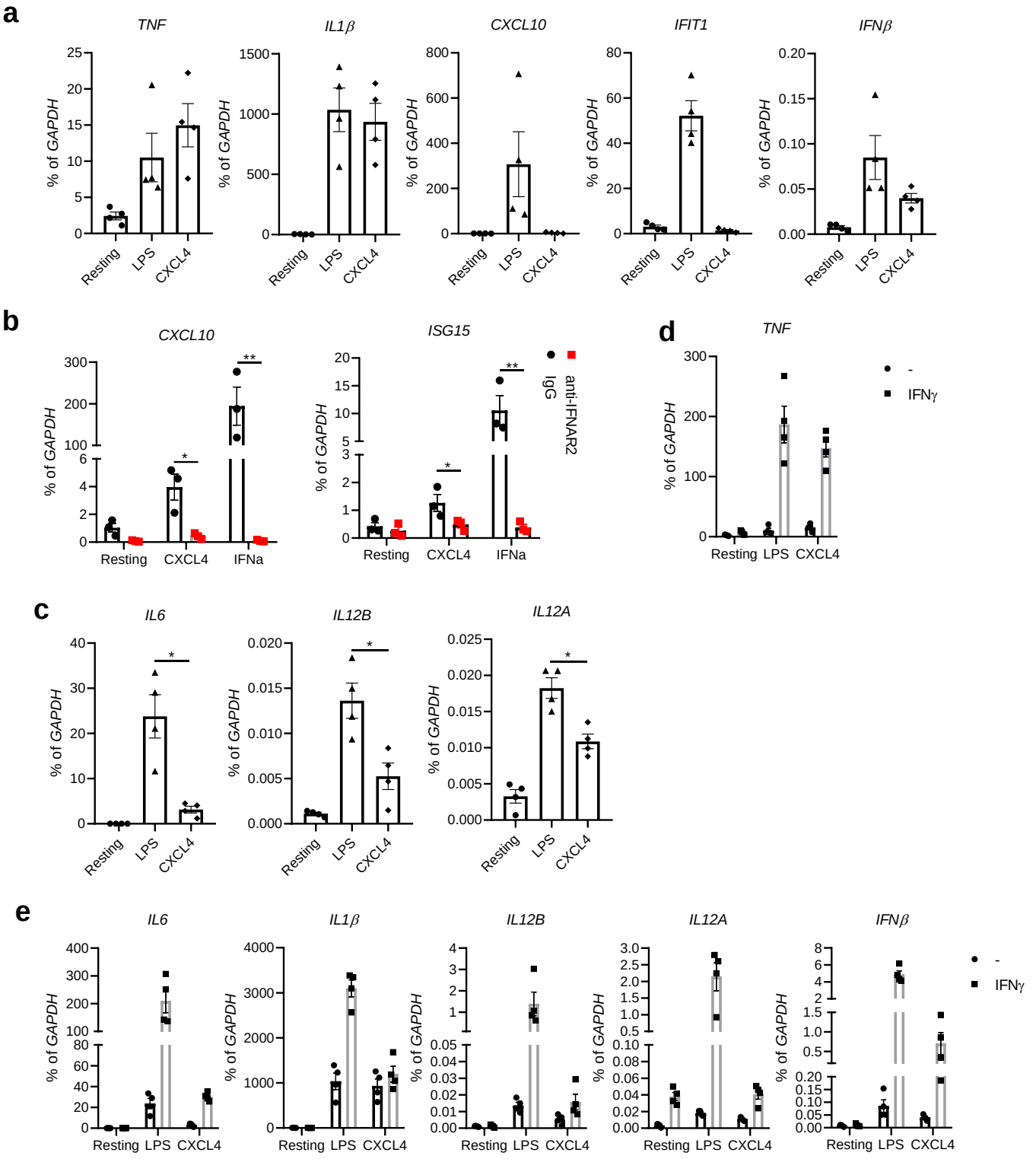

Yang et al., Fig. 6

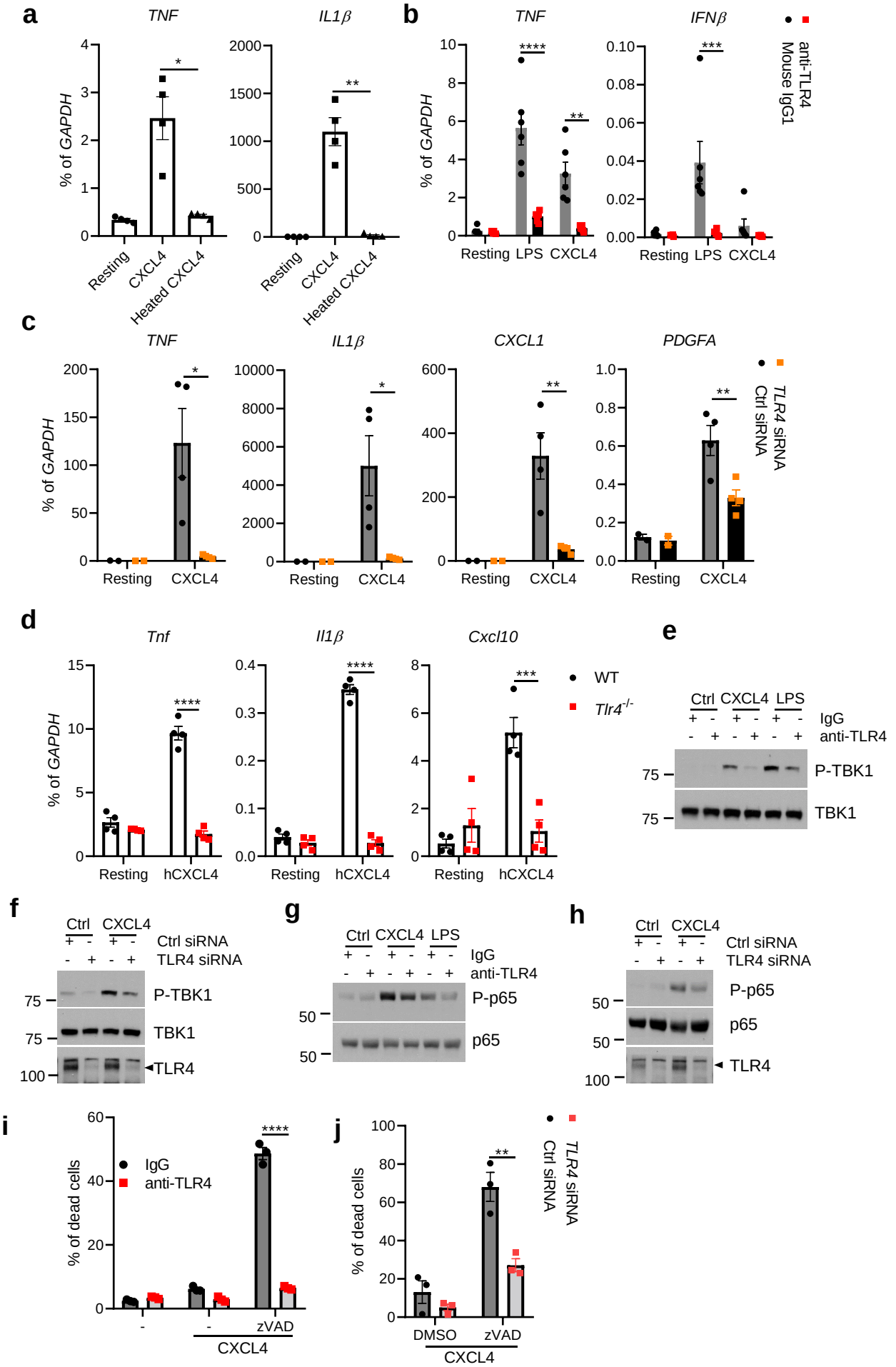
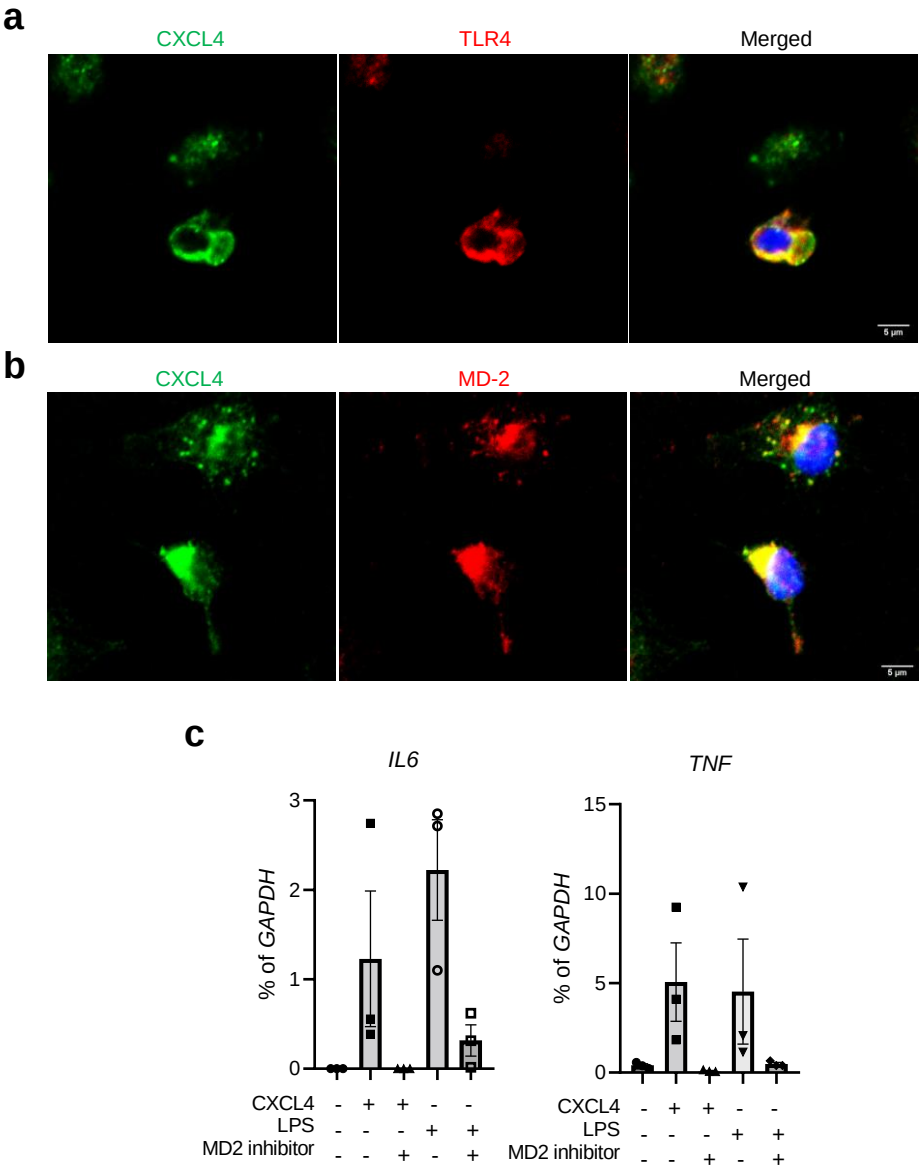
Yang et al., Fig. 7